CHALLENGES TO FINDING OLIVINE ON THE SURFACE OF 4VESTA. A. W. Beck[1], J. M. Sunshine[2], T. J. McCoy[1], T. Hiroi[3]. [1]Smithsonian Institution (becka@si.edu), [2]University of Maryland, [3]Brown University.

Introduction: One of the primary goals of the Dawn mission, which is currently in orbit around the asteroid 4Vesta, is to further the understanding of the differentiation of that asteroid. Identifying olivine-rich lithologies on Vesta can constrain different petrologic scenarios, which result in varied olivine distributions. For example, in a magma ocean fractionation scenario, olivine may be expressed as a uniform, Mg-rich, deep-seated harzburgitic (Hzbg: Ol + Opx) mantle lithology [1]. However, if olivine-rich lithologies formed via fractionation in multiple crustal plutons, more heterogeneously distributed, relatively shallow and ferroan Hzbg cumulates are expected [2]. Aiding in deciphering the geologic history of Vesta are the HED (howardite, eucrite, diogenite) meteorites, a voluminous group of achondrites that likely originated from that asteroid [3].

In the past 20 years, an increasing number of Hzbg diogenites have been described in the meteorite collection. Recent studies support the interpretations that Hzbg diogenites are fractionated cumulates that they are co-genetic with the olivine-free, orthopyroxenitic (Opxn) diogenites, which comprise the majority of the diogenite group [2,4]. It remains unclear whether these Hzbg cumulates represent initial cumulates from a global magma ocean, or cumulates from multiple crustal plutons. A key observation by Dawn in resolving this issue will be identifying and mapping the distribution of Hzbg diogenite-like terranes on Vesta.

VIR, a visible-near infrared spectrometer aboard Dawn, is the primary instrument for mapping the surface mineralogy of Vesta [5]. Discriminating the broad 1-μm olivine absorption feature from those features in pyroxene requires the spectral range and resolution of VIR. While mineralogical differences between Hzbg and Opxn diogenites have been well defined [2], spectral variations between these two lithologies have not been examined. In this work, we compare the visible-near infrared spectral properties of two Hzbg diogenites to an Opxn diogenite to test their ability to be distinguished within the spectral range and resolution provided by VIR.

Methods: Hzbg diogenites are very heterogeneous in olivine distribution, e.g. [1], [6], [7], and single thin-section modes are not representative of whole samples. We calculated average modal olivine abundances for Hzbg diogenites where multiple thin-section modes have been reported. The mean olivine abundance for Hzbg diogenites is ~10-30% (Fig. 1). Two Hzbg diogenites within this range were selected for this work:

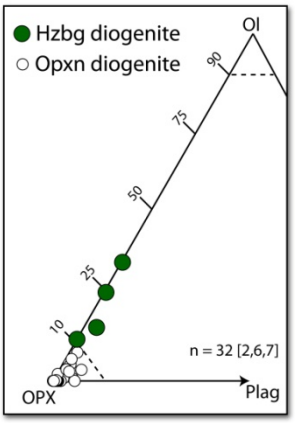

Fig. 1. Classification diagram for diogenites. Opxn points are single-section modes, Hzbgs are a mean of multiple sections.

MIL 07001 (MIL: 10% Ol) and GRA 98108 (GRA: 25% Ol). Thin-section analyses of each sample were used to confirm previous modes and descriptions. Approximately 250 mg sample splits were acquired for spectral analysis. The splits were coarsely crushed and examined using an E-SEM to confirm thin-section mineralogy. Coarsely crushed splits were then ground to < 45 μm powders and analyzed using the visible-near infrared (VNIR) spectrometer at RELAB. The RELAB spectrum of Opxn diogenite Tathouine was used for comparison. Tathouine was selected because of its lack of olivine [6], relative homogeneity, lack of weathering (observed fall), and because its spectrum was collected under similar analytical conditions to those used here.

Results and Discussion: *Petrology.* MIL differs from other Hzbg diogenites in three ways: 1) Most olivine grains are small, 2) opaques are > 1 vol.%, and 3) no plagioclase is observed (Fig. 2a). Orthopyroxenes in this sample are Wo_1 En_{76}, olivines are Fo_{72}. The mode is Opx 88%, Ol 10%, Plag 0%, and opaques 2% (Fig. 2a). Thin section observations of GRA,5 are consistent with [2], where section ,16 was examined. GRA,5 has large orthopyroxene and olivine grains, though portions of the section have smaller, equigranular textures, similar to MIL (Fig. 2b). Orthopyroxene and olivine compositions in GRA,5 are the same as

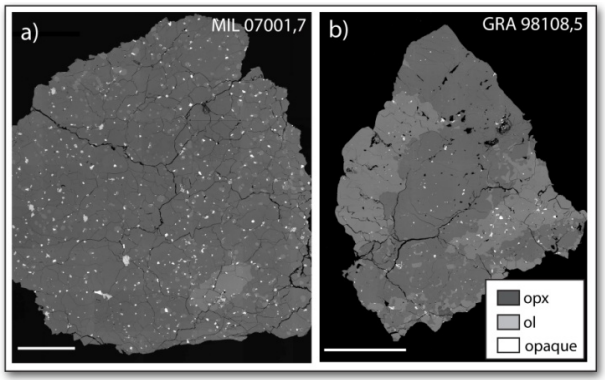

Fig. 2. BSE maps of two Hzbg diogenites, 2 mm scale bars.

those in section,16 (Wo_2 En_{76}; Fo_{73}). The mode of GRA,5 is Opx 67%, Ol 32%, Plag 1%, and opaques <1%, slightly more Ol-rich than section ,16 (Ol 19%). High calcium pyroxene (HCP) is found only as an accessory phase in both GRA and MIL.

E-SEM Observations. We assume an olivine abundance of ~25% for the GRA split, which is a mean between previously reported modes [1,7] and this study. E-SEM observations of the coarsely ground GRA split generally support this mineralogy. Olivine abundance has not been reported in other sections of MIL, so mean olivine abundance was not assumed for that split. The equigranular texture and homogeneous distribution of olivine in MIL (Fig. 2a), however, suggest uniform olivine distribution; thus we assume 10% olivine for the split. E-SEM observations generally support this assumption.

VNIR Spectra. In orthopyroxene-dominated samples, like the diogenites, the addition of olivine should shift the 1-μm orthopyroxene absorption feature towards longer wavelengths, visibly broaden the 1.4-μm feature, and if abundant enough, change the relative band strengths of the 1- vs. 2- μm features. The additions of HCP and plagioclase, along with variations in orthopyroxene end-member compositions and grain size, can also have effects on VNIR spectra of diogenite-like materials [8], some of which can be misinterpreted to indicate the presence of olivine [9]. However, orthopyroxenes in the samples being compared here have nearly identical end-member compositions (~Wo_1 En_{76}). Similarly, all samples contain negligible HCP, plagioclase and opaques, and powders were similar grain sizes. Therefore, olivine abundance, in which these samples differ, is the only variable that would affect VNIR absorption features.

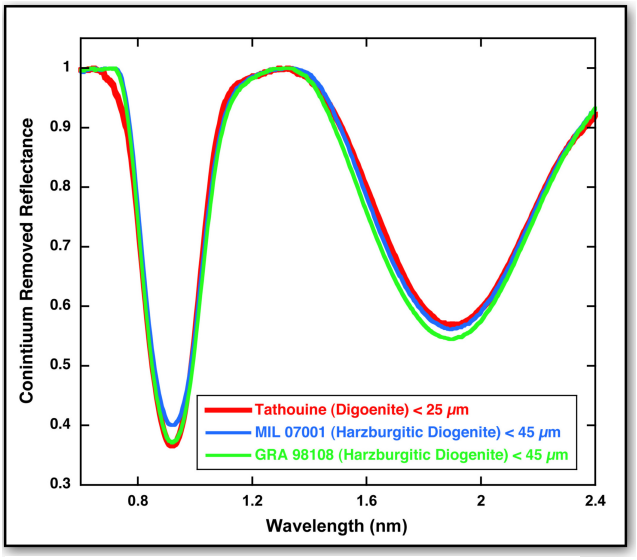

Fig. 3. VNIR spectra of Hzbg and Opxn diogenites.

We do not see visible evidence of olivine in VNIR spectral range from the two Hzbg samples. Instead, GRA and MIL show well developed ~1- and 2-μm absorption features, and are indistinguishable from the spectrum of the olivine-free Opxn diogenite, Tathouine (Fig. 3). Thus, at olivine abundances up to ~25%, olivine is not visibly detectable in these spectra. This is consistent with previous work on binary mixtures [10]. More quantitative estimates are ongoing.

Conclusions: When compared using high-resolution laboratory spectroscopy, Hzbg diogenite meteorites with 10-25% olivine are indistinguishable from olivine-free, Opxn diogenite meteorites in the VNIR spectral range. If olivine-rich cumulates on Vesta have similar olivine abundances to the Hzbg diogenites, which is presumable, the VIR instrument on Dawn will likely have difficulty distinguishing those rocks from the surrounding olivine-free, Opxn terranes. Therefore, a lack of observation of olivine-rich terranes on the surface of Vesta [11] may not be an indication that they are absent. It is possible that dunitic lithologies (90% Ol) may be exposed on the surface of Vesta [12]. However, given the paucity of representative samples in the meteorite collection relative to the Hzbgs, dunites are not likely to comprise a significant portion of olivine-rich terranes exposed on the surface of Vesta.

GRaND, a Gamma Ray and Neutron Detector onboard Dawn, may be able to distinguish Hzbg diogenites with 10-25% Ol from Opxn diogenites on Vesta through the use of elemental mixing models [13], though the coarse spatial resolution of the instrument will present challenges to these observations. If GRaND can accurately discern between Hzbg and Opxn diogenite-like terranes on the surface of Vesta, than this instrument may be an essential tool in resolving one of the fundamental questions about Vestan differentiation.

References: [1] Righter K. & Drake M.J. (1996) *Icarus* 124:513-529. [2] Beck A.W. & McSween H.Y. (2010) *MAPS* 45:850-872. [3] McSween H.Y. et al. (2011) *Space Sci. Rev.* 163:141-174. [4] Mittlefehldt D.W. et al. (2012) *MAPS* 47:72-98. [5] De Sanctis M.C. et al. (2011) *Space Sci. Rev.* 163:321-369. [6] Bowman L.E. et al. (1997) *MAPS* 32:869-875; [7] Righter K. (2001) *LPSC XXXII* #1765. [8] Gaffey M.J. et al. (2002) Asteroids III 183-204. [9] Mayne R.G. et al. (2011) *Icarus* 214:147-160. [10] Cloutis et al. (1986) *JGR* 91:11,641-11,653. [11] De Sanctis M.C. et al. (2012) *LPS XLIII*. [12] Beck A.W. et al. (2011) *MAPS* 46:1133-1151. [13] Prettyman T.H. et al. (2011) *Space Sci. Rev.* 163:371-459.